Choi, S. O., New techniques for estimating the shut-in pressure in hydro- fracturing pressure-time curves.
International Symposium on the Fusion Technology of Geosystem Engineering, Rock Engineering and Geophysical Exploration
Seoul, Korea, Nov. 18-19, 2003

New techniques for estimating the shut-in pressure in hydro-fracturing pressure-time curves

Sung O. Choi
Korea Institute of Geoscience and Mineral Resources, Daejeon, Korea

Abstract: A definite shut-in pressure in hydraulic fracturing techniques is needed for obtaining the correct information on the in-situ stress regimes in rock masses. The relation between the behaviour of hydraulically induced fractures and the condition of remote stress is considered to be major reasons of an ambiguous shut-in pressure in hydraulic fracturing pressure-time history curves. This paper describes the results of a series of numerical analyses carried out using UDEC(Universal Distinct Element Code, Itasca), which is based on the discrete element method, to compare several methods for determining the shut-in pressure during hydraulic fracturing. The fully coupling of hydraulic and mechanical analysis was applied, and the effects of four different discontinuity geometries in numerical modelling have been investigated for this purpose. The effects of different remote stress regimes and different physical properties on hydraulic fracture propagation have been also analyzed. Several methods for obtaining shut-in pressure from the ambiguous shut-in curves have been applied to all the numerical models. The graphical intersection methods, such as (P vs. t) method, (P vs. log(t)) method, (log(P) vs. log(t)) method, give smaller values of the shut-in pressure than the statistical method, (dP/dt vs. P). Care should be taken in selecting a method for shut-in pressure, because there can be existed a stress anomaly around the wellbore and fracturing from the wellbore by a constant flow rate may have a more complicate mechanism.

1. Introduction

The hydraulic fracturing technique used first for the well stimulation in the petroleum industry is currently applied for determining the principal stresses in the Earth's crust after Hubbert and Willis (1957). The basic concept for the determination of the principal stresses starts from several assumptions that the rock mass is an impermeable, homogenous, and isotropic elastic material and one of the principal stresses is parallel to the direction of wellbore. Consequently the other principal stresses are assumed to be on the plane perpendicular to the wellbore and calculated from the pressure-time data obtained during hydraulic fracturing (Haimson, 1968).

While calculating the principal stresses from the pressure-time history graph, however, the accurate determination of shut-in pressure, which shows a pressure decline gradually after stopping the fluid injection, is very important because the shut-in pressure is equal to the normal stress acting on the induced hydraulic fractures and indicates the minimum horizontal principal stress directly (Aamodt and Kuriyagawa, 1983, and Rummel, 1987).

However, in most field cases the pressure-time history after shut-in shows an ambiguous curve rather than a sharp break, so a lot of methods for determining the shut-in pressure have been proposed. Some compare the several shut-in pressures obtained from several methods for more accurate determination of the minimum horizontal principal stress. A review of these various methods can be found in Kim and Flanklin (1987), Lee and Haimson (1989) and Amadei and Stephansson (1997). They describe the strengths and weaknesses of each method by comparing the shut-in pressures, but were not able to propose which method is best for determining the minimum horizontal principal stress. Because nobody knows exactly the minimum horizontal principal stress in the Earth's crust, the errors between the real value and the calculated value could not be defined.

In this study, an attempt has been made to validate the several proposed methods for shut-in pressure, under various remote stress regimes and various rock properties using numerical modeling techniques. In particular, numerical analyses have been carried out to investigate:

1. the effects of the different numerical geometries on the hydraulic and mechanical behaviors of the rock masses;
2. the effects of the different remote stress regimes on the fluid flow and the fracture propagation;
3. the effects of the different rock properties on the hydraulic and mechanical behaviors of the rock masses; and
4. the comparison of each shut-in pressure calculated by the various proposed methods with the known applied remote stresses.

2. The Numerical Model

The numerical analyses were carried out using the program UDEC (Universal Distinct Element Code, Itasca, 1993). UDEC is a commercial program based on the discrete element method (DEM), and the whole model is generated by a number of distinct blocks, which can be divided into deformable triangular finite difference zones in UDEC.

Moreover, the deformation of the discontinuous rock masses consists of the elastic and plastic deformation of blocks of intact rock, together with displacements along and across discontinuities. The blocks were considered to be elasto-plastic with a Mohr-Coulomb failure criterion and a non-associated flow rule. This allowed the rock blocks themselves to deform plastically. The discontinuities were assumed to be elasto-plastic with a Coulomb slip criterion, and they were treated as boundary conditions between blocks, and both large displacements along discontinuities and rotations of blocks were allowed.

UDEC has the capability to perform the analysis of fluid flow through the discontinuities of a system of impermeable blocks. A fully coupled mechanical and hydraulic analysis enables us to interpret the relation between the deformation of rock mass and the hydraulic conductivity of the block system. In this case, flow is governed by the pressure differential between adjacent domains.

The flow rate is calculated in two different ways, depending on the type of contact of each block. For a corner-to-edge contact, the flow rate is:

$$q = -k_c \Delta p \tag{1}$$

where k_c is a contact permeability factor and Δp is a fluid pressure differential between adjacent domains.

In case of an edge-to-edge contact, the flow rate is given by the following equation using the cubic law of flow in discontinuities (Witherspoon et al., 1980).

$$q = -k_j a^3 \frac{\Delta p}{l} \tag{2}$$

where k_j is a joint permeability factor, a is the contact hydraulic aperture, and l is the contact length.

The hydraulic aperture a is given, in general, by:

$$a = a_0 - u_n \tag{3}$$

where a_0 is the joint aperture at zero normal stress, and u_n is the joint normal displacement which is controlled by the normal stress and the rock properties. A minimum value, a_{res}, is assumed for the aperture, below which mechanical closure does not affect the contact permeability. Where the hydraulic pressure exceeds the normal stress acting on discontinuities, it is possible to open them so that the aperture is larger than a_0. Consequently, a compressive effective stress will cause apertures partly to close while a zero effective stress will allow them to open to a width greater than a_0.

Model geometry and input data

In order to simulate the hydraulic fractures propagating from a wellbore and interpret the normal stress acting on the hydraulic fractures, a two-dimensional horizontal plane strain section, which is orthogonal to the vertical wellbore, was used in our numerical models. The modeled area was 10.0 m by 10.0 m, with a wellbore 0.2 m in diameter as shown in Fig. 1. The outer boundary was considered to be large enough against the boundary effect in the numerical studies.

In our numerical model, this horizontal plane strain section was assumed subject to the far-field stress regimes. Consequently, the minor horizontal principal stress S_h is acting up-and-down on the model, and the major horizontal principal stress S_H is right-and-left, as shown in Fig. 1. At the same time, the vertical principal stress S_v was considered to be applied normal to the two dimensional model. S_v might be neglected in a plane strain numerical model but was intended to represent a K-value, the ratio of the average horizontal principal stress to the vertical principal stress. For our entire numerical analyses, S_h is set equal to 10 MPa and S_v is set equal to 12.5 MPa, which is intended to represent a depth of about 500 m.

To examine the pattern of the induced hydraulic fractures around a wellbore subject to different far-field stress regimes, S_H was set equal to 1.0, 1.25, or 1.5 times S_h for different models. When S_H was set equal to 1.5 times S_h in magnitude, the applied K-value was 1.0, with the condition $S_h < S_v < S_H$. The physical parameters used in the analysis are given in Table 1, which represents the average properties of a limestone.

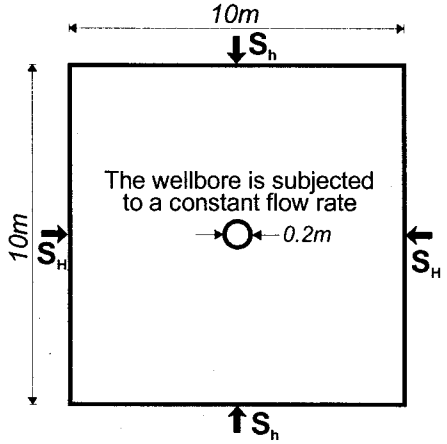

Fig. 1. Plan view of modeled zone and applied boundary condition.

Table 1. Physical properties used in the numerical analysis.

	Value	Units
Block property		
Density	2600	kg m^{-3}
Bulk modulus	15.6	GPa
Shear modulus	11.7	GPa
Cohesion	28.4	MPa
Tensile strength	10.0	MPa
Friction angle	35.2	degree
Discontinuity property		
Joint normal stiffness	70.8	GPa m^{-1}
Joint shear stiffness	58.8	GPa m^{-1}
Cohesion	28.4	MPa
Tensile strength	10.0	MPa
Friction angle	35.2	degree
Residual aperture	0.020	mm
Zeronormal stress aperture	0.068	mm

Preliminary analysis on different types of joint sets

In general, it has been known that rock masses consist of intact rock and discontinuities such as faults, joints and bedding planes, and the presence of such discontinuities in rock masses dominates the response of jointed rock masses to static or dynamic loading (Goodman, 1976; Chen, 1998). For representation of these discontinuities in numerical modeling, the joints in rock masses are treated as individual elements termed joint elements in the FEM or BEM. In the FDM, joints in rock masses are treated as slidelines, even though these treatments can only be applied when the number of joints and their displacements are small. The DEM, on the other hand, was proposed by Cundall (1971) and specially designed to solve discontinuity problems, and represents a rock mass as an assemblage of discrete intact blocks and discontinuities as interfaces between blocks. Blocks can be moved, rotated or deformed, and the interfaces may be compressed, opened or slipped. Therefore, it can treat non-linearity that may arise from large displacement, rotation, slip, and separation of the medium.

In our studies, we are concerned about the numerical propagation of the hydraulically induced fractures in rock masses. Even though the joints in rock masses were not considered in our numerical models, however, it was concluded from the above reasons that a program based on the DEM should be adopted in our numerical studies for our future researches on the fracture propagation in jointed rock masses.

UDEC represents a rock mass as an assemblage of discrete blocks, and cannot make a new discontinuity except opening the existing discontinuities between blocks during the numerical simulations. Therefore, the pattern of an assemblage of blocks should be decided before simulating the hydraulic fractures propagation. This explains that each discontinuity, which has been generated for the representation of discrete blocks, will be a path for the hydraulic fractures propagation. For this purpose, every discontinuity was glued to each other and had same physical properties to intact rock blocks.

Fig. 2 shows four different assemblages of blocks used in our numerical models, and shows a possible pattern of block assemblages. From the different analyses on different block assemblages, it was anticipated which type of block assemblages is suitable for demonstrating the hydraulic fractures propagation. For all the cases shown in Fig. 2, the physical properties were same as those in Table 1 and the far-field stresses were S_h=10 MPa, S_H=15 MPa, and S_v=12.5 MPa, with a constant flow rate of 1 *l*/sec from the wellbore.

As shown in Table 1, the properties for joint cohesion, joint tensile strength, and joint friction angle were set equal to those of block properties. This means that the entire joint sets in Fig. 2 are glued and used as a path for fracture propagation in the intact rock masses, as mentioned above.

When the discontinuity geometry was generated in the simple two orthogonal sets as shown in Fig. 2(a), the hydraulic fractures developed perpendicular to S_h from the wellbore in a single line. This might be expected, and the fracture propagation pattern was too simple to be considered numerically (Fig. 3(a)). Moreover, in case of (b) and (c) of Fig. 2, the fracture propagation couldn't show a certain direction (Fig. 3(b) and (c)). The randomly sized polygonal joint sets shown in Fig. 2(d) were proved to be a most proper discontinuity geometry to investigate the pattern of hydraulic fractures propagation subject to the different remote stress regimes (Fig. 3(d)). Because the

case (b) and (c) of Fig. 2 did not show the hydraulic fracture propagation pattern, which should be dominated by the differential horizontal principal stress. The case (d) showed the almost same results as those from the laboratory studies of Choi and Lee (1995). They suggested that the hydraulic fractures, generated in the cubic block of 30 x 30 x 30 cm, did not show a straight line and developed to a branch of fractures, not to a single line.

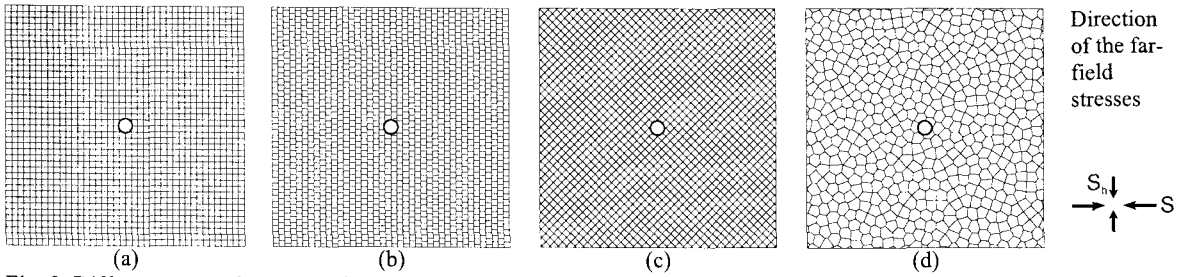

Fig. 2. Different types of an assemblage of blocks and joints; (a) Simple two orthogonal joint sets, (b) Staggered joint sets, (c) Two diagonal joint sets, and (d) Randomly sized polygonal joint sets.

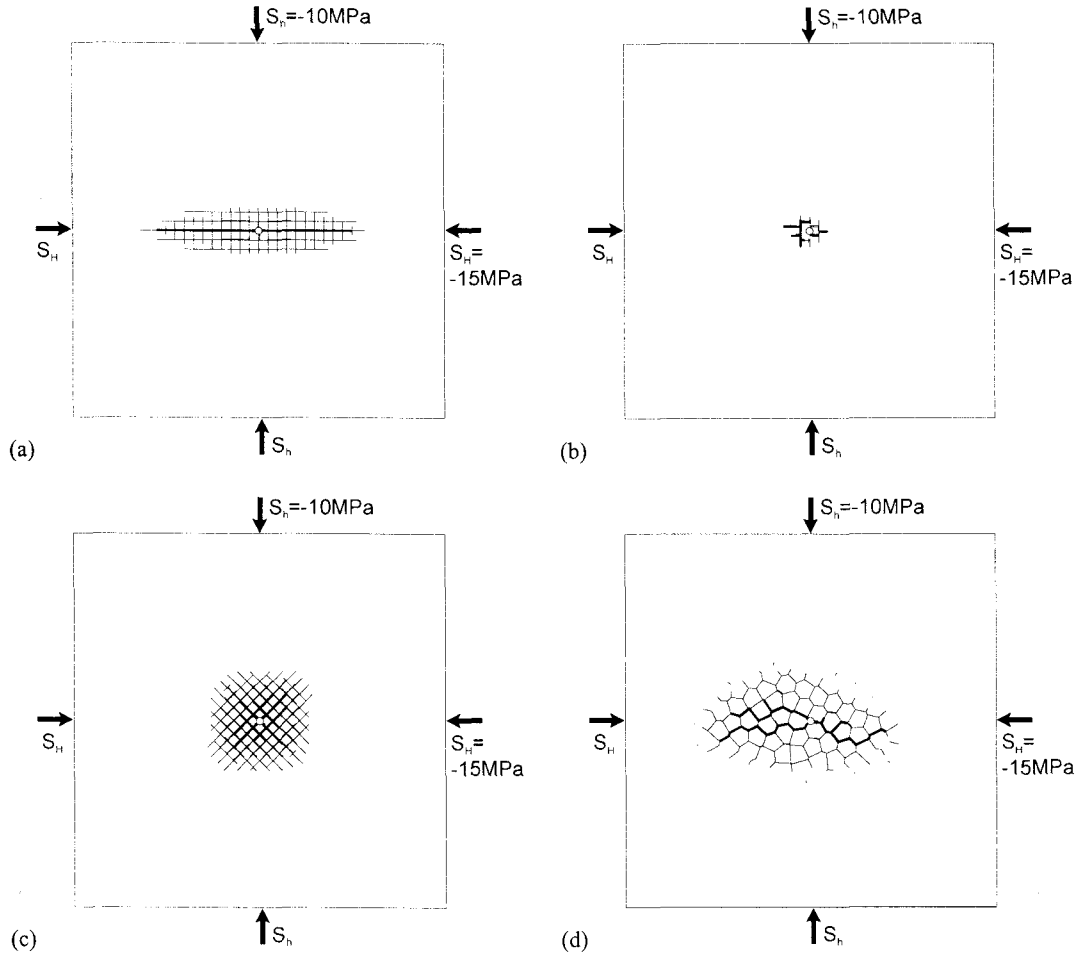

Fig. 3. Hydraulic fracture propagation attitude in the simple two orthogonal joint sets (a), the staggered joint sets (b), the two diagonal joint sets (c), and the randomly sized polygonal joint sets (d). (Thin lines around wellbore denote the infiltration of fluid from wellbore, and thick lines denote the hydraulic fractures generated from wellbore)

Randomly sized polygonal joint geometry with different remote stress regimes

From the preliminary analysis on different discontinuity sets for model geometry, it was decided that the randomly sized polygonal joint geometry is very realistic for simulating the hydraulic fractures propagation. For all the next numerical modeling, the pressure in the wellbore was traced as a function of the flow-time while the wellbore was subjected to a constant flow rate.

Fig. 4 shows one of examples obtained from numerical studies. The constant flow rate of 1 *l*/sec was applied into the wellbore until the breakdown occurred, and then set to zero after breakdown.

The pressure-time history curve in Fig. 4 shows a traditional breakdown pressure and shut-in pressure. Therefore, the attempt to validate the several proposed methods for shut-in pressure, under various remote stress regimes and various rock properties, will be possible using this numerical modeling technique.

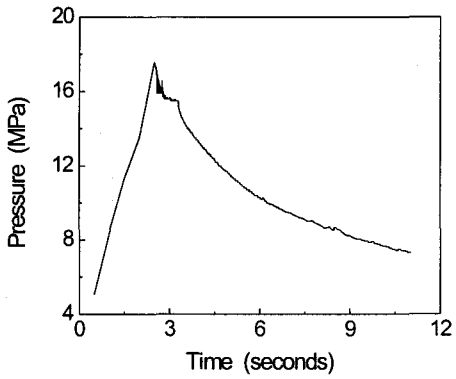

Fig. 4. Pressure-time history curve obtained from numerical analysis.

Different remote stress regimes were applied using the randomly sized polygonal discontinuity sets. Fig. 3(d) shows hydraulic fracture propagation and fluid infiltration into the rock mass during hydraulic fracturing for the case of K = 1.0, that is, S_H = 15 MPa applied with the fixed value of S_h = 10 MPa and S_v = 12.5 MPa. And Fig. 5 shows the fracture propagation pattern for the case of K = 0.8 and 0.9, that is, S_H = 10 MPa and S_H = 12.5 MPa, respectively.

Fig. 3(d) and Fig. 5 show different hydraulic fractures propagation and fluid infiltration around the wellbore under the action of different values of differential stress (S_H–S_h).

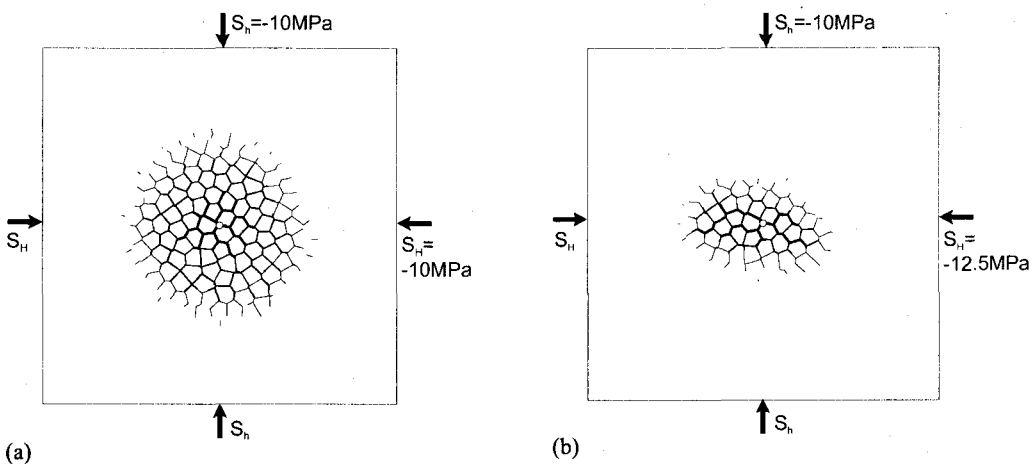

Fig. 5. Hydraulic fracture propagation pattern for different remote stress regimes; (a) S_h = S_H = 10 MPa and S_v = 12.5 MPa (K=0.8), (b) S_h = 10 MPa and S_H = S_v = 12.5 MPa (K=0.9). (Thin lines around wellbore denote the infiltration of fluid from wellbore, and thick lines denote the hydraulic fractures generated from wellbore).

When the horizontal stress state was isotropic ($S_H = S_h = 10$ MPa, see Fig. 5(a)), the hydraulic fractures developed in a radial direction. As the applied differential stress was increased (Fig. 5(b) and Fig. 3(d)), however, the hydraulic fractures trend sub-normal to S_h and the infiltration of the pressurized fluid is great in the direction of S_H. It reveals that the differential stress plays obviously a critical role in controlling hydraulic fracture propagation within modeled rock masses. And one can anticipate that this tendency on hydraulic fracture propagation should rise with the increase of the differential stress.

Comparison of several methods for determination of shut-in pressure

The determination of the shut-in pressure is straightforward when a sharp break is observed in the pressure-time curve after the initial fast pressure decline following pump shut-off. However, in many situations the pressure decay is gradual with no obvious breaks or kinks and the shut-in pressure cannot be readily defined. For these reasons, a number of methods have been proposed for estimating the shut-in pressure from pressure-time curves. In this study, the four most frequently used methods were adopted for comparison.

The first one is the inflection point method, which consists of first drawing a tangent to the pressure versus time curve following shut-in, proposed by Gronseth & Kry (1983). The second one is the semi-logarithmic representation method, proposed by Doe et al. (1983), and the third one is the log-log representation method that was first suggested by Zoback and Haimson (1982). And the final one is the bilinear pressure decay rate method of Tunbridge (1989). This method has now become the most popular method for the determination of the shut-in pressure (Lee and Haimson, 1989; Amadei and Stephansson, 1997).

Fig. 6 shows examples for determination of the shut-in pressure from the various methods. In this case, the calculated shut-in pressure can vary by as much as 9%. For the Basalt Waste Isolation Project in Hanford, Washington, Aggson and Kim (1987) found that the shut-in pressure (assumed equal to the minimum horizontal stress) could vary by as much as 4.9 MPa (14%), and for the Äspo nuclear waste disposal project in Sweden, the variation was about 2.1 MPa (38%) (Amadei and Stephansson, 1997).

The values of the shut-in pressure for different rock properties and different remote stress regimes determined by the various methods are summarized in Table 2. Analysis of this table reveals that the bilinear decay rate method gives generally the highest values of shut-in pressure. According to Amadei and Stephansson (1997), the inflection method gives the highest values, the pressure decay method yields the next largest values, and the intersection method gives the smallest values of the shut-in pressure. In our analysis, it is revealed that the determination of shut-in pressure using the various methods shows the same trend as their suggestion, even though the inflection method was not considered.

Comparing the results from Test 1, 2, and 3, none of the shut-in pressures show the exact minimum horizontal principal stress applied (S_h = 10 MPa). This is indicative of the relative effects of differential stress around the wellbore. In other words, as can be known in the classic Kirsch solution (Jaeger and Cook, 1979), which defines the radial and circumferential stress distributions around a cylindrical hole in an infinite isotropic elastic medium under plane strain conditions, the stresses around a wellbore depend on their point at polar coordinate as well as the magnitude of far field stresses. From the stress contour map in equilibrium states before hydraulic fractures were generated, the stress in the direction of x-axis at the wellbore wall, showed 10 MPa equal to the applied far-field stress. But it shows a gradual increase with radial distance from the wellbore.

According to Zhang et al. (1996 and 1999), the maximum circumferential stress occurs near the wellbore and is about 1.5 or 1.85 times the far-field stress, and significant stress redistribution occurs within the central area about 2.5 times the diameter of the wellbore. In our cases, the maximum circumferential stress was about 1.2 or 1.4 times the far-field stress, and the hydraulic fractures have propagated to a considerable distance from the wellbore. Therefore, the calculated shut-in pressures indicated the stress acting on the whole fracture surfaces.

Nonetheless, the shut-in pressures obtained from the bilinear pressure decay rate method are still the highest value and exceed the maximum circumferential stress around the wellbore. One should apply careful consideration in using the bilinear pressure decay rate method for determination of the shut-in pressure, even though this method is currently the most popular.

From the results of Test 4 and 5, to investigate the effects of cohesion on determination of shut-in pressure, it reveals that the cohesion value does not affect the magnitude of the shut-in pressure. This situation is same in Test 6 and 7, which are to investigate the effects of tensile strength on determination of shut-in pressure. However, the different values of joint normal stiffness and joint shear stiffness can affect the shut-in pressure as shown in the result from Test 8. These parameters simply denote the virtual connection mode between each block; namely, normal stiffness for spring element and shear stiffness for slide element. As mentioned previously, our model has a number of discontinuities, but these are not indicative of actual joints. Our discontinuities in model were used only to build

a numerical model. Therefore, different result from different joint stiffness applied does not have a considerable meaning. However, when the hydraulic fracture propagation in jointed rock masses is considered for numerical simulation, the joint normal and shear stiffness on actual joint sets should be applied.

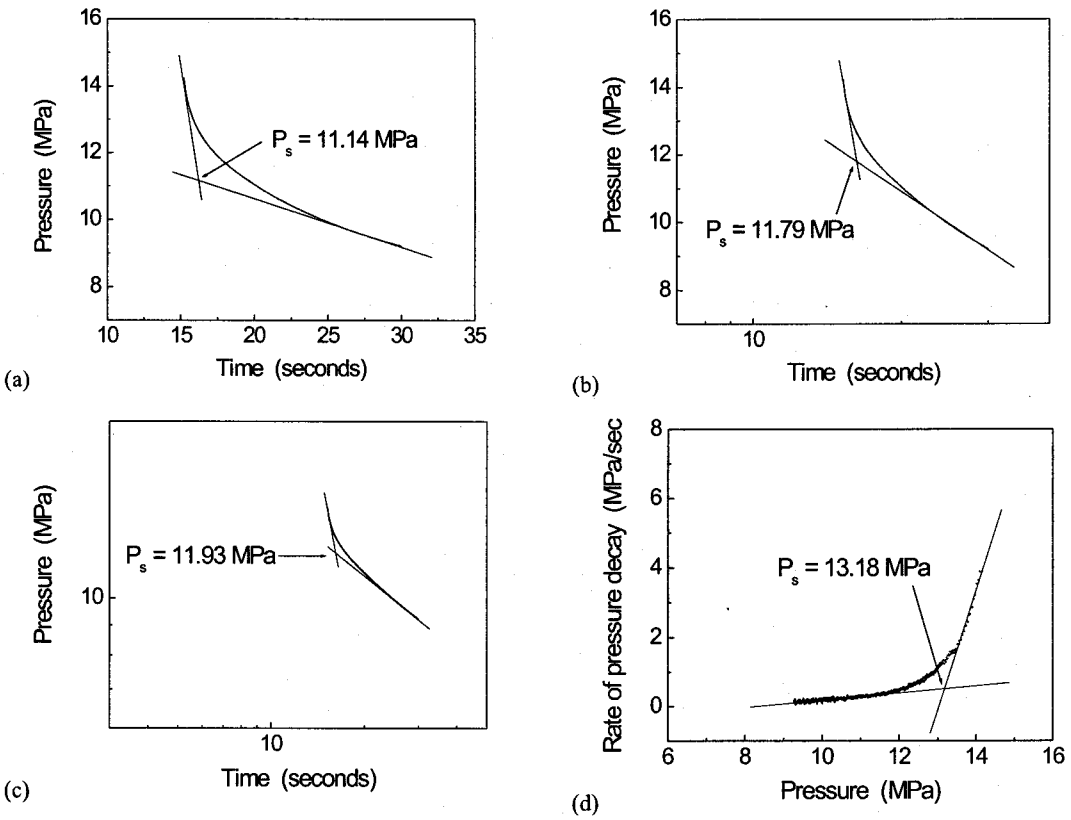

Fig. 6. Determination of shut-in pressure P_s from hydraulic fracturing pressure versus time records: (a) tangent intersection method, (b) pressure versus log(time) method, (c) log(pressure) versus log(time) method, and (d) bilinear pressure decay rate method.

Table 2. Values of the shut-in pressure for different rock properties and remote stress regimes, determined by the various methods.

		P_s (MPa)							
Relationship	*Method*	*Test 1*	*Test 2*	*Test 3*	*Test 4*	*Test 5*	*Test 6*	*Test 7*	*Test 8*
P vs. t	Intersection	11.89	12.70	12.89	12.67	12.57	13.18	13.41	11.14
P vs. log(t)	Intersection	12.08	12.77	13.54	13.35	13.47	14.14	14.09	11.79
Log(P) vs. log(t)	Intersection	12.01	12.84	14.06	13.88	13.95	14.85	14.81	11.93
dP/dt vs. P	Bilinear decay rate	11.90	13.28	15.83	16.00	15.88	15.51	15.44	13.18
Mean value		11.97	12.90	14.08	13.98	13.97	14.42	14.44	12.01

1) Test 1, 2, and 3 are for S_H = 10 MPa, 12.5 MPa, and 15 MPa, respectively. (S_v is fixed to 12.5 MPa and S_h to 10 MPa, and rock properties are same to those shown in Table 1)
2) Test 4 and 5 are for the various cohesion values. (Double cohesion value in Test 4, and five times cohesion value in Test 5. The remote stress regimes and the other rock properties are same to the case of Test 3)
3) Test 6 and 7 are for the various tensile strength values. (Double tensile strength value in Test 6, and five times cohesion value in Test 7. The remote stress regimes and the other rock properties are same to the case of Test 3)
4) Test 8 is the obtained shut-in pressures when the joint normal stiffness and joint shear stiffness were applied as a double value of Test 3.

3. Conclusions

Several methods for determination of the shut-in pressure in hydraulic fracturing have been investigated using the numerical code UDEC.

The results of the numerical analyses have revealed that the differential stresses can play an important role in propagating the hydraulic fractures and infiltrating the pressured fluid into the rock masses, and the shut-in pressure obtained from the bilinear pressure decay rate method was larger than that of the other intersection methods.

(1) From the preliminary analysis on different discontinuity geometries in model, it was revealed that the randomly sized polygonal joint geometry is most realistic for hydraulic fracturing, rather than the orthogonal geometry or the diagonal geometry.

(2) The history of the wellbore pressure during the simulation of hydraulic fracturing showed a traditional hydraulic fracturing pressure-time curve, and enabled us to investigate the mechanism of hydraulic fracturing numerically. The randomly sized polygonal discontinuities were glued to be indicative of the intact rock mass, and opened and closed by the fluid flow using the hydraulic and mechanic coupling.

(3) The results of the analyses on different remote stress regimes have confirmed that the differential stress plays a critical role in controlling hydraulic fractures propagation within the intact rock masses; namely, hydraulic fractures developed in a radial direction when the horizontal stress state was isotropic. As the applied differential stress was increased, the hydraulic fractures sub-normal to S_H closed more than those sub-normal to S_h, and the infiltration of the pressurized fluid sub-normal to S_H decreased more than those sub-normal to S_h.

(4) The shut-in pressures obtained from the bilinear pressure decay rate method were larger than those from the other intersection methods. Thus care should be taken in using the bilinear pressure decay rate method for determination of the shut-in pressure, even though this method is currently popular.

(5) The results of numerical studies on different rock properties revealed that the rock properties do not affect the magnitude of the shut-in pressure.

References

Aamodt, L. and Kuriyagawa, M., 1983, Measurement of instantaneous shut-in pressure in crystalline rock, Proc. Hydraulic Fracturing Stress Measurements, Monterey, National Academy Press, Washington, DC, 139-142.

Aggson, J.R. and Kim, K., 1987, Analysis of hydraulic fracturing pressure history: a comparison of five methods used to identify shut-in pressure, Int. J. Rock Mech. Min. Sci. & Geomech. Abstr., 24, 75-80.

Amadei, B. and Stephansson, O., 1997, Rock stress and its measurement, Chapman & Hall, pp.121-199.

Chen, S.G. and Zhao, J., 1998, A study of UDEC modelling for blast wave propagation in jointed rock masses, Int. J. Rock Mech. Min. Sci. & Geomech. Abstr., 35, 93-99.

Choi, S.O. and Lee, H.K, 1995, The analysis of fracture propagation in hydraulic fracturing using artificial slot model, Tunnel & Underground, J. of Korean Society for Rock Mechanics, Vol.5, 251-265.

Cundall, P.A., 1971, A computer model for simulating progressive large scale movements in blocky rock systems, Pros. Symp. Int. Soc. Rock Mech., Nancy, France, Vol.1, paper II-8.

Doe, T.W. et al., 1983, Determination of the state of stress at the Stripa Mine, Sweden, Proc. Hydraulic Fracturing Stress Measurements, Monterey, National Academy Press, Washington, DC, 119-129.

Goodman, R.E., 1976, Methods of geological engineering in discontinuous rocks, West publishing, St. Paul.

Gronseth, J.M. and Kry, P.R., 1983, Instantaneous shut-in pressure and its relationship to the minimum in-situ stress, Proc. Hydraulic Fracturing Stress Measurements, Monterey, National Academy Press, Washing-ton, DC 55-60.

Haimson, B.C., 1968, Hydraulic fracturing in porous and nonporous rock and its potential for determining in situ stresses at great depth, PhD Thesis, Univ. of Minnesota, 234p.

Hubbert, K.M. and Willis, D.G., 1957, Mechanics of hydraulic fracturing, Petrol. Trans. AIME, T.P. 4597, 210, 153-166.

Itasca, 1993, Universal Distinct Element Code (UDEC) Version 3.0, Itasca Consulting Group Company.

Jaeger, C. and Cook, N.G., 1979, Fundamentals of rock mechanics, Chapman and Hall, London.

Kim, K. and Franklin, J.A. (coordinators), 1987, Suggested methods for rock stress determination, Int. J. Rock Mech. Min. Sci. & Geomech. Abstr., 24, 53-73.

Lee, M.Y. and Haimson, B.C., 1989, Statistical evaluation of hydraulic fracturing stress measurement parameters Int. J. Rock Mech. Min. Sci. & Geomech. Abstr., 26, 447-456.

Rummel, F., 1987, Fracture mechanics approach to hydraulic fracturing stress measurements, in Atkinson, B. K., eds., Fracture Mechanics of Rocks, Academic Press, London, pp.217-239.
Tunbridge, L.W., 1989, Interpretation of the shut-in press-ure from the rate of pressure decay, Int. J. Rock Mech. Min. Sci. & Geomech. Abstr., 26, 457-459.
Witherspoon, P.A., Wang, J.S.Y., Iwai, K., Gale, J.E., 1980, Validity of cubic law for fluid flow in a deformable rock fracture, Water Resour. Res. 16, 1016-1024.
Zhang, X., Sanderson, D.J., Harkness, R.M., Last, N.C., 1996, Evaluation of the 2-D permeability tensor for fractured rock masses, Int. J. Mech. Min. Sci. & Geomech. Abstr., 33, 17-37.
Zhang, X., Last, N., Powrie, W., Harkness, R., 1999, Numerical modelling of wellbore behaviour in fractured rock masses, J. Pet. Sci. & Eng., 23, 95-115.
Zoback, M.D. and Haimson, B.C., 1982, Status of hydraulic fracturing method for in situ stress measurements, Proc. 23rd US Symp. Rock Mech., Berkeley, SME/ AIME, 143-156.